Total scattering cross sections calculations for Electron impact on CF2 radical

AVANI BAROT[1*], DIVYESH BHAVSAR[2], MAYURI BAROT[3]

[1] Sigma Institute of Science, Bakrol, Waghodia, Vadodara-390019, Gujarat, India

[2]Bhavan's Sheth R. A. College of Science, Khanpur, Ahmedabad-380001,Gujarat, India

[3] Government Science College, Gandhinagar-382016, Gujarat, India

*E-mail: barot_avani29@yahoo.com

Abstract

Total scattering cross sections for electron impact on CF2 in the gas phase are presented from 0.1 eV to 2000 eV. Computation of such e - CF2 cross sections over such a wide range of energy is reported for the first time employing two distinct formalisms. From 0.1 eV to the ionization threshold of the target we employed the ab-initio R-matrix method, while at higher energies we used the Spherical Complex Optical Potential (SCOP) method. At the crossing point, the two theories match one another quite well and hence prove that they are consistent with one another. A quantum chemistry code is utilized to generate the target properties which are in good agreement with earlier reported data. The calculations show a peak at 0.81 eV using the Static Exchange Polarization (SEP) model and at 1.86 eV using a Static Exchange (SE) model which is a reflection of the formation of a Π_u shape resonance state. These values are close to theoretical calculations by Rozum et al. [J. Phys. Chem. Ref. data, 35, 267 (2006)] with a peak at 0.89 eV for SEP model and 1.91 eV for SE model. Lee et al. [Phys. Rev. A, 74, 052716 (2006)] have also reported a peak at 1.65 eV. The total cross sections presented here are in good agreement with other experimental and theoretical calculations. These results show that the techniques employed here can be used to predict cross sections for other targets for which data is scarce or not available. This methodology maybe integrated into online databases such as the Virtual Atomic and Molecular Data Centre (VAMDC) to provide cross section data required by many desperate users.

Key Words: R-matrix method, ab-initio calculations, Spherical Complex Optical Potential, Total cross sections, CF2.

PACS number(s): 34.80.Bm

I INTRODUCTION

Molecular radicals play an important role in many electron-driven processes, including radiation damage in tissue, gas discharges, low-temperature plasma etching environments and waste deposition technologies. In particular, radicals of the fluorocarbons play a significant role in the etching processes and evolution of plasmas used in micro and nano-structure assembly, for example it is now well established that the concentration of CFx (x = 1–3) radicals have a significant effect on the behavior of fluorocarbon plasmas [1, 2]. Such CFx radicals are predominantly formed by electron impact induced dissociation of the fluorocarbon feed gases.

In this paper we study the scattering of CF2 radical on electron impact. Experimental studies of electron collision cross sections with CF2 are difficult and hence to date measured data has only been reported by one group [3]. Francis-Staite et al. [3] used a crossed–beam electron scattering experiment to measure e -CF2 differential cross sections at specific angles (20° – 135°) for incident energies between 2 and 20 eV. They also reported calculated data for absolute differential cross sections and integral cross sections using the Schwinger multichannel method for impact energies between 2 and 20 eV. Earlier Maddern et al. [4] reported absolute differential cross sections for incident electron energies of 30–50 eV and over an angular range of 20o–135o.

Theoretical investigations of the total elastic cross sections for e -CF2 scattering have been reported by four groups [3, 5-7]. Lee et al. [5] used the Iterative Schwinger variational method and calculated elastic differential, integral and momentum transfer cross sections as well as total absorption cross sections in the energy range 1 – 500 eV. Rozum et al. [6] used the R-matrix method to evaluate the total elastic and excitation cross sections of the six lowest lying electronic excited states of the CF2. Antony et al. [7] have reported total elastic and total inelastic cross sections using a Spherical Complex Optical Potential for impact energies between 50 and 2000 eV. Owing to the difficulties involved in experiments with CF2 radicals, total ionization cross sections have been reported experimentally by two groups, Huo et al. [8] and Tarnovsky et al. [9] while theoretical estimates of the total ionization cross sections are reported by three groups [7,10,11]. Thus, reviewing the literature, it is quite clear that the work on e -CF2 is scarce, as most of the authors have focused their results over a specific range of impact energies as well as for specific cross sections. This work reports various cross section data for a wide energy range which can be used for plasma modeling.

This paper reports electron impact excitation, differential, momentum transfer, ionization and total cross sections for e -CF2 scattering over a wide range of energy starting from a very low energy of 0.1 eV to 2000 eV. Electron-molecule collision cross sections from very low energy up to threshold play an important role in determining electron transport properties and electron energy distribution of a swarm of electrons drifting through various gases. They also play significant role in modeling low temperature plasmas. In addition to the practical interest, electron scattering data are of fundamental theoretical importance towards the understanding of various electron assisted molecular chemistry [12]. The motive behind such study is twofold; (1) to study the resonance processes which are more prominent at low impact energies below 10 eV through which knowledge of dissociative electron attachment and negative ion formation can be gathered and (2) to compare the results of this work with available data. In order to achieve these goals we employed two different formalisms that are consistent and widely used over specific ranges of impact energies. For low impact energies up to the ionization threshold of the target we employ the ab-initio R-matrix method [13] while at higher energies computation of the total cross sections is carried out using a quantum mechanical approach through Spherical Complex Scattering Potential [14, 15].

This paper is organized as follows, in Section 2 we describe first the target model and then describe the salient features of theoretical methodologies employed for low energy as well as high energy calculations. Section III is devoted to results and discussions of the results obtained and finally we end up with conclusions of the present study.

II THEORETICAL METHODOLOGIES

The energy range of this study (0.1 to 2000 eV) cannot be modeled by any single theoretical formalism. Hence the present calculations are based on two distinct methodologies, one valid below the ionization threshold of the target and the other above it. This paper reports low energy (0.1 eV to about 15 eV) ab-initio calculation using the Quantemol-N package [16] employing the UK molecular R-matrix code [13] and the Spherical Complex Scattering Potential formalism above 15 eV. The target model plays an important role as its correct representation ensures accuracy and stability in the calculation, therefore before discussing the scattering formalisms we must discuss the target model employed.

A Target Model Used For Low-Energy Calculations

According to equilibrium geometry, CF2 is a triangular radical with a C–F bond length of 2.45 a0 and a bond angle F–C–F of 104.98o [17]. We employed a double zeta plus polarization (DZP) basis set similar to 6-31G for the target wave function representation and assumed C2v point group symmetry of order four. For the optimized nuclear geometry of the target we employed second order Möller-Plesset perturbation theory in the 6–31G (d) basis set and the occupied and virtual molecular orbitals obtained using Hartree–Fock–Self consistent field (HF–SCF) optimization which was used to set up the CF2 electronic target states. The ground state Hartree–Fock electronic configuration is 1b22, 1a12, 2a12, 3a12, 2b22, 4a12, 3b22, 5a12, 1b12, 1a22, 4b22 and 6a12. To establishing a balance between the amount of correlation incorporated in the N-electron target representation, φNi, and the (N+1) electron scattering wavefunction in our configuration integration (CI) model, out of 24 electrons, we froze 16 electrons in ten molecular orbitals (1a1, 2a1 3a1, 4a1, 5a1, 1b1, 1b2, 2b2, 3b2, 1a2). The remaining 8 electrons were allowed to move freely in the active space of 6 target occupied and virtual molecular orbitals (6a1, 7a1, 2b1, 3b1, 4b2, 5b2).

TABLE I. Target properties for CF2 molecule.

Properties of Target	Present	Theoretical Results	Experimental Results
Ground state energy (Hartree)	– 236.7341	– 236.7305 [Ref.5] – 236.7275 [Ref.18]	-----
First excitation energy (eV)	3.28	2.49 [Ref.6] 2.42 [Ref.19] 2.46 [Ref.20]	2.30 [Ref.3]
Rotational constant (cm-1) (A)	2.95	2.83 [Ref.6]	2.95 [Ref.17] 2.947 [Ref.21]
(B)	0.403		0.417 [Ref.21]
(C)	0.353		0.364 [Ref.21]
Dipole moment (D)	0.301	0.246 [Ref.5] 0.440 [Ref.18] 0.448 [Ref.6]	0.469 [Ref.21]

Our self-consistent field (SCF) calculation yielded the ground state energy for CF2 as –236.7341 Hartree which is in good agreement with –236.7305 Hartree calculated by Lee et al. [5] and –236.7575 Hartree of Russo et al. [18]. The nuclear coordinates will determine the molecular orbitals, rotational constants, dipole moment and symmetries of the molecule. These parameters highly affect the cross section (differential, momentum transfer and total cross sections) calculations. Hence it is imperative to use proper nuclear coordinates. The calculated rotational constants for CF2 are 2.95 cm-1, 0.403 cm-1 and 0.353 cm-1 which are very close with measured data of 2.947 cm-1, 0.417 cm-1 and 0.364 cm-1 reported by Kirchhoff et al. [21] and also same as 2.95 cm-1 reported in Computational Chemistry Comparison and Benchmark Data Base [17] and is slightly lower than the theoretical value of 2.83 cm-1 reported by Rozum et al. [6]. The calculated first excitation energy is 3.28 eV is higher compared to measured value of 2.3 eV reported by Francis-Staite et al. [3] and theoretical values of 2.49 eV reported by Rozum et al. [6], 2.42 eV reported by Cai [19]. The calculated dipole moment is 0.301 D which is higher compared to 0.246 D reported by Lee et al. [5] but is lower than the experimental value of 0.469 D of Kirchhoff et al. [21] and the theoretical value of 0.44 D of Russo et al. [18] and 0.448 D of Rozum et al. [6]. The target properties along with available comparisons are listed in Table I and the eight electronic excitation thresholds for CF2 are listed in Table II.

TABLE II. Vertical excitation energies for e -CF2.

State	Energy (eV)	State	Energy (eV)
1A1	00.00	1A2	11.06
3B1	03.28	3B2	11.45
1B1	06.14	1B2	12.66
3A2	10.96	3A1	12.99

b Low Energy Scattering Formalism (0.1 eV To ~ 15 eV)

The most popular methodologies employed for low energy electron collision calculations are the Kohn variational method [22], the Schwinger multichannel method [23] and the R-matrix method [24], of which the R-matrix is the most widely used method. The underlying idea behind the R-matrix method relies on the division of configuration space into two spatial regions, namely an inner region and outer region. The spatial R-matrix spherical boundary is chosen such that the complete electronic charge distribution of the target electrons plus the scattering electron is embedded in it. Thus the all N target electrons plus one scattering electron are contained in the inner region which makes the problem numerically complex, but physically very precise. All short range interactions between the target electrons and scattering electron are dominant in this region which includes static, exchange and correlation polarization potentials. Consequently the accuracy of scattering calculation depends critically on how appropriately the inner region physics is defined. The solution of the inner region problem

involves rigorous quantum chemistry methods and thus consumes most of the time needed for calculation. However, the inner region problem is solved independently of the energy of the scattering electron and hence is done only once.

In the outer region where the scattering electron is at large distance from the center of mass of the target, the probability of swapping its identity with any one of the target electrons is negligible, resulting in a negligible contribution from the exchange and correlation effects. This makes the problem very simple since only multipolar interactions between the scattering electron and the target are included. A single center close coupling approximation with direct potentials leads to a set of coupled differential equations and this allows quick, simple and fast solutions in the outer region. The outer region calculations are repeated for each set of energies. In the present calculation the inner R-matrix radius is taken as 10 a0. In the outer region the R-matrix on the boundary is propagated to a sufficiently large distance where the interaction between target electrons and scattering electron is assumed to be zero. In the present case this distance is 100 a0. Asymptotic expansion techniques are used to solve the outer region functions [24].

In the inner region target electrons are placed in some combination of target molecular orbitals which are represented by Gaussian-type orbitals and these are multiplied by spin functions to generate configuration state functions (CSF's). The target molecular orbitals are also supplemented by a set of continuum orbitals which have longer range such that they extend beyond the inner region R-matrix boundary and hence the inner region wave function is constructed using a close coupling approximation [25] for all N+1 electrons. In the close coupling method, scattering cross sections are calculated including the effect of Polarization and in the presence of resonances due to formation of transient negative ions and various threshold effects. The total wave function for the system is expressed as,

$$\psi_k^{N+1} = A\sum_I \psi_I^N(x_1,\Lambda\ ,x_N)\sum_j \zeta_j(x_{N+1})a_{Ijk} + \sum_m \chi_m(x_1,\Lambda\ ,x_{N+1})b_{mk} \tag{1}$$

where A is the anti–summarization operator that takes care of exchange effect among N+1 electrons, xN (rn, σn) is the spatial and spin coordinate of the nth electron, ξj is a continuum molecular orbital spin-coupled with the scattering electron. aIjk and bmk are variational coefficients determined by the diagonalization of N+1 Hamiltonian matrix.

The accuracy of the calculation depends solely on the accurate construction of the wave function given in equation (1). The first summation runs over the target states used in the close-coupled expansion and a static exchange calculation has a single Hartree-Fock target state in the first sum. Here one electron is placed in the continuum orbital of the target and the rest of the electrons move in available target molecular orbitals thus generating target + continuum configurations. In the second term χm are multi-center quadratically integrable functions, known as L2 functions constructed from target occupied and virtual molecular orbitals, and are used to represent correlation and Polarization effects. This sum runs over the minimal number of configurations, usually 3 or fewer, required to relax orthogonality constraints between the target molecular orbitals and the functions used to represent the configuration. The continuum orbitals are centered on the center of mass of the molecule. The present close-coupled calculation uses the lowest number of target states, represented by a configuration interaction (CI) expansion in the first term and over a hundred configurations in the second. These configurations allow for both orthogonality relaxation and short-range Polarization effects.

The complete molecular orbital representation in terms of occupied and virtual target molecular orbitals are constructed using the Hartree-Fock Self-Consistent Field method with Gaussian-type orbitals (GTOs) and the continuum orbitals of Faure et al. [26] and included up to g (l = 4) orbitals. The benefit of employing a partial wave expansion for low energy electron molecule interaction is its rapid convergence. In the case of dipole-forbidden excitations ($\Delta J \neq 1$), where J represents the rotational quantum number, the convergence of the partial waves is rapid but in the case of dipole-allowed excitations $(\Delta J = 1)$ the partial wave expansion converges slowly due to the long range nature of the dipole interaction. In order to account for the higher partial waves not included in the fixed nuclei T-matrices, the born correction is applied. The effect of partial waves higher than l = 4 were included using a Born correction which requires expressions for the partial waves as well as full Born cross sections. These expressions were drawn from the work of Chu and Dalgarno [27]. We were constrained to employ partial waves for the continuum orbital up to l = 4 only, as the representation in Gaussian type orbitals for the Bessel functions higher than l = 4 were not available. For low partial waves $(l \leq 4)$ T matrices computed from

the R-matrix calculations are employed to compute the cross sections. The low partial wave contributions arising from the Born contribution are subtracted in order that the final cross section set only contains those partial waves due to the R-matrix calculation. We have performed the calculations with and without dipole Born corrections.

The R-matrix provides the link between the inner region and the outer region. The R-matrix is propagated to an asymptotic region where the radial wave-functions describing the scattering electron can be matched to analytical expressions. For this purpose the inner region is propagated to the outer region potential until its solution matches with the asymptotic functions given by the Gailitis expansion [28]. Coupled single center equations describing the scattering in the outer region are integrated to identify the K-matrix elements. The K-matrix is a symmetric matrix whose dimensions are the number of open channels. All the observables can be deduced from it and it can be used to obtain T-matrices using the definition,

$$T = \frac{2iK}{1 - iK} \tag{2}$$

These T-matrices are in turn used to obtain various total cross sections. The K-matrix is diagonalized to obtain the eigenphase sum. The eigenphase sum may be further used to obtain the position and width of resonances by fitting them to the Breit Wigner profile [29]. Differential and Momentum transfer cross sections (MTCS) are calculated using POLYDCS program [30]. In fact the MTCS is obtained by integrating the differential cross sections (DCS) with a weight factor (1-cosθ).

C The high energy scattering formalism

Even with the latest computing facilities available the R–matrix code cannot be extended to scattering calculations beyond about 15 to 20 eV hence if intermediate to high energy electron scattering is to be modeled we must use the well–established SCOP formalism [31, 32]. We employ partial wave analysis to solve the Schrödinger equation with various model potentials as input. The interaction of incoming electron with the target molecule can be represented by a complex optical potential comprising of real (VR) and imaginary parts (VI) ,

$$V_{out}(E_i, r) = V_R(E_i, r) + iV_I(E_i, r) \tag{3}$$

such that,

$$V_R(r, E_i) = V_{st}(r) + V_{ex}(r, E_i) + V_p(r, E_i) \tag{4}$$

where, the real part VR comprises of static potential (Vst), exchange potential (Vex), and Polarization potential (Vp). The static potential, (Vst) arises from Coulombic interactions between the static charge distribution of the target and projectile. It is calculated at the Hartree–Fock level. The exchange potential (Vex) term accounts for electron exchange interaction between the incoming projectile and one of the target electrons. The Polarization potential (Vp) represents approximately short range correlations and long range Polarization effects arising from the temporary redistribution of the target charge cloud. Note that the SCOP as such does not require any fitting parameters. The most important basic input for evaluating all these potentials is the charge density of the target. We have used the atomic charge density derived from the Hartree Fock wave functions of Bunge et al. [33]. Any e –molecule system is more complex compared to any e -atom system but this complexity is reduced by adopting a single center approach [34, 35] so as to make a 'spherical approximation' applicable. In case of CF_2 we reduce the system to single centre by expanding the charge density of both carbon and fluorine atoms at the center of mass of the system by employing the Bessel function expansion detailed in Gradshetyn and Ryzhik [36]. The spherically averaged molecular charge–density $\rho(r)$, is determined from the constituent atomic charge density using the Hartree Fock wave functions of Bunge et al. [33]. The molecular charge density $\rho(r)$ obtained is then renormalized to incorporate the covalent bonding [37]. In the SCOP method the spherical part of the complex optical potential is treated exactly by a partial wave analysis to yield various cross sections [38]. Here we have neglected the non-spherical terms arising from the vibrational and rotational excitations in the full expansion of the optical potential.

The atomic charge densities and static potentials (Vst) are formulated from the parameterized Hartree–Fock wave functions given by Bunge et al. [33]. The parameter free Hara's 'free electron gas exchange model' [39] is used to generate the exchange potential (Vex). The Polarization potential (Vp) is constructed from the parameter free model of the correlation–Polarization potential given by Zhang et al. [40]. Here, various multipole

non-adiabatic corrections are incorporated into the intermediate region which will approach the correct asymptotic form at large 'r' smoothly. In the low energy region, the small 'r' region is not important due to the fact that higher–order partial waves are unable to penetrate the scattering region. However in the present energy region, a large number of partial waves contribute to the scattering parameters and correct short range behavior of the potential is essential.

The imaginary part in Vopt is called the absorption potential, and Vabs or VI accounts for the total loss of flux scattered into the allowed electronic excitation or ionization channels. Vabs is not a long range effect and its penetration towards the origin increases with increasing energy. This implies that at high energies the absorption potential accounts the inner-shell excitations or ionization processes that may be closed at low energies.

The well-known quasi-free model form of Staszeweska et al. [41, 42] is employed for the absorption part and is given by,

$$V_{abs}(r,E_i) = -\rho(r)\sqrt{\frac{T_{loc.}}{2}}\left(\frac{8\pi}{10k_F^3 E_i}\right)\theta(p^2 - k_F^2 - 2\Delta)(A_1 + A_2 + A_3) \tag{5}$$

where the local kinetic energy of the incident electron is,

$$T_{loc} = E_i - (V_{st} + V_{ex} + V_p) \tag{6}$$

where p2 = 2Ei, kF= [3π2 $\rho(r)$]1/3 is the Fermi wave vector and A1, A2 and A3 are dynamic functions that depend on $\theta(x)$, I, Δ and Ei. I is the ionization threshold of the target, $\theta(x)$ is the Heaviside unit step–function and Δ is an energy parameter below which Vabs= 0. Hence, Δ is the principal factor which decides the value of total inelastic cross section, since below this value ionization or excitation is not permissible. This is one of the main characteristics of the Staszeweska model [41, 42]. In the original Staszeweska model [41, 42] $\Delta = I$ and hence it ignores the contributions coming from discrete excitations at lower incident energies. This had been realized earlier by Garcia and Blanco [43] who elaborately discussed the need to modify Δ value. In our calculations we have treated Δ as a slowly varying function of Ei around I. Such an approximation is meaningful since Δ fixed at I would not allow molecular excitation at energies $E_i \le I$. If Δ is taken as being much lower than the ionization threshold then Vabs, becomes unexpectedly high near the peak position so in order to overcome this we give a reasonable minimum value of 0.8I to Δ [35] and express the parameter as a function of Ei around I as follows,

$$\Delta(E_i) = 0.8I + \beta(E_i - 1) \tag{7}$$

The value of the β parameter is obtained by requiring that Δ = I (eV) at Ei= Ep, the value of incident energy at which Qinel reaches its peak. Ep can be found by calculating Qinel by keeping Δ = I. Beyond Ep, Δ is kept constant and is equal to the ionization threshold, I. The theoretical basis for assuming a variable Δ is discussed in more detail by Vinodkumar et al. [35].

The complex optical potential thus formulated is used to solve the Schrödinger equation numerically through a partial wave analysis. This calculation will produce complex phase shifts for each partial wave which carries a signature of the interactions of the incoming projectile with the target. At low impact energies only a few partial waves are significant, but as the incident energy increases, more partial waves are needed for convergence. The phase shifts (δ_l) thus obtained are employed to find the relevant cross sections, the total elastic (Qel) and the total inelastic cross sections (Qinel) using the scattering matrix $S_l(k) = \exp(2i\delta_l)$ [44]. Total cross sections such as the total elastic (Qel) and the total inelastic cross sections (Qinel) can be derived from the scattering matrix [44]. The sum of these cross sections will then give the total scattering cross section (QT).

III RESULTS AND DISCUSSION

In this study we have carried out comprehensive computations of the total cross section produced by the collision of electrons with CF2 in the gas phase from 0.01 eV to 2000 eV. Both of the theoretical formalisms used have their own limits over the range of impact energies. More elaborately, the ab-initio calculations are computationally viable only up to around 20 eV, while the SCOP formalism can be employed successfully from threshold of the target to 2000 eV. In this work we compute the total cross section below the ionization threshold using a close coupling formalism employing the R-matrix method where total cross section is obtained as sum of total elastic and total electronic excitation cross sections while beyond ionization threshold we use the SCOP formalism and the total cross section is obtained as the sum of the total elastic and inelastic cross sections. The results we obtained are consistent and there is a smooth transition at the overlap of two formalisms (around 14 eV). Thus it is possible to provide the total cross section over a wide range of impact energies from meV to keV. We have presented our results in graphical form and numerical values are tabulated in Table III.

TABLE III. Total cross sections (TCS) for e - CF2 scattering in (Å2)

Energy (eV)	TCS (Å2) Q-mol	Energy (eV)	TCS (Å2) SCOP
0.1	23.64	12.0	16.65
0.3	21.95	15.0	15.06
0.5	25.95	20.0	13.80
0.7	59.47	25.0	13.23
0.8	77.79	30.0	12.93
1.0	34.40	50.0	12.33
1.06	30.01	60.0	12.04
2.0	18.86	70.0	11.70
3.0	16.59	80.0	11.29
4.0	15.22	90.0	10.85
5.0	14.46	100.0	10.43
6.0	13.81	300.0	5.81
7.0	13.22	500.0	4.19
8.0	12.91	700.0	3.34
9.0	12.91	1000.0	2.58
10.0	13.34	1500.0	1.89
11.0	14.18	2000.0	1.50

Figure 1 shows a comparison of the present total cross section for e -CF2 scattering for 0.1 eV to 20 eV. We performed calculations using static exchange (SE) and static exchange plus Polarization (SEP) models. Our data is compared with the theoretical data of Rozum et al. [6] Lee et al. [4] and Francis Staite et al [3] and experimental data of Francis staite et al. [3] and recommended data of Yoon et al. [45].

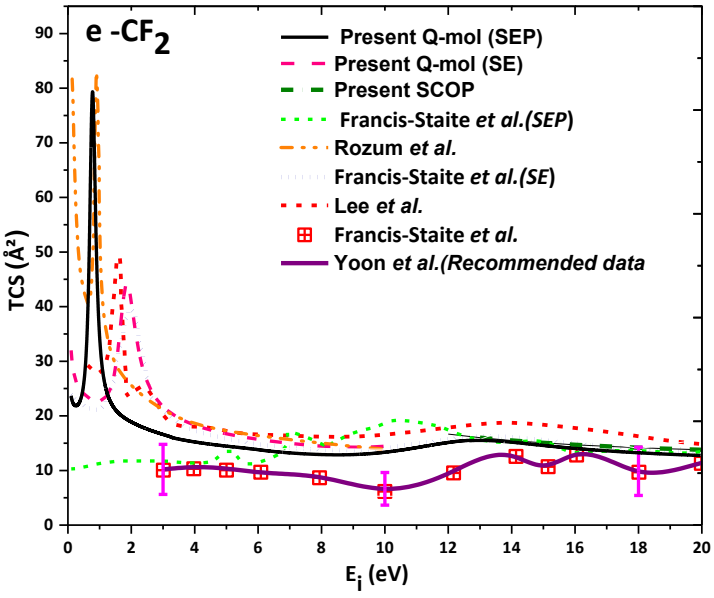

Fig. 1. (Color online) Total cross section for e -CF2 scattering. Black solid line: Present Q-mol results (SEP); Dash line: Present Q-mol results (SE); Dash dot line: Present SCOP results; Short Dash: Francis-Staite et al. (SEP) [3]; Dash Dot Dot line: Rozum et al. [6] (SEP); Short dash line: Francis-Staite et al. (SE) [3]; Short Dash line: Lee et al. [5]; Open Square: Francis-Staite et al. [3]; Solid circle: Yoon et al. [45]

Rozum et al. [6] have also performed R-matrix calculations using SE and SEP models. We obtained a prominent peak of 79.20 Å2 at 0.82 eV in the SEP model and 44.20 Å2 at 1.86 eV from the SE model which is a reflection of Π_u shape resonance state. This shift (0.79 eV to 1.04 eV) in the peak is attributed to the attractive nature of Polarization potential which improves the results. The theoretical results of Rozum et al. [6] shows peak value of 80.64 Å2 at 0.89 eV for SEP model and 39.57 Å2 at 1.91 eV for SE model which are in excellent agreement with our results both qualitatively as well as quantitatively. Overall there is good agreement of our results with the results of Rozum et al. [6] throughout their reported range. The theoretical SEP results of Francis Staite et al [3] do not show first shape resonance at low energy but their SE results show resonance at 2.02 eV with a peak of 39.98 Å2 which is close to present value at 1.86 eV with a slightly higher peak of 44.20 Å2. The SE results of Francis Staite et al.[3] are in good agreement with our results beyond 3 eV. Finally the theoretical results of Lee et al. [5] reported a peak at 1.65 eV with magnitude of 49.3 Å2. The shape resonance peak of Lee et al. [5] is slightly shifted compared to all other reported SEP data. Beyond 3 eV their data are slightly higher compared all data presented here. The low energy shape resonance structure is not visible in the available experimental as the experimental data reported by Francis Staite el al. [3] is from 2 eV to 20 eV and the shape resonance occurs below 2 eV. We also observed another small structure at 13.42 eV in our low energy total cross section results which is also seen at the same energy in the data of Lee et al. [4]. This structure is also reflected in the experimental result of Francis-Staite et al. [3] at 10.35 eV. This is due to 2B2 scattering channel. The experimental data of Francis-Staite et al. [3] and recommended data of Yoon et al. [45] are lower compared to all theoretical results. This discrepancy in ICS is due to the fact that they obtained their ICS data by integrating the DCS data which introduces an error of 45% due to extrapolation of DCS data in the range 20o to 0o and from 135o to 180o. However our data show very good agreement with the experimental data of Francis Staite et al. [3] beyond 15 eV. There is smooth crossover of the our R matrix data with SCOP data at around 14 eV.

In Figure 2 we present a comparison of our total cross section data over a wide energy range from 0.1 eV to 2000 eV. The data over such a wide range is an amalgamation of data obtained through the two formalisms, R-matrix and SCOP. The data obtained through R-matrix and SCOP agrees and confirms a smooth transition at around 14 eV from one methodology to the other. We have not shown our SE data and SE data of Francis Staite et al. [3] and Rozum et al. [6] in Figure 2 as they are already discussed in Figure 1. Also we have already discussed the low energy data (up to 20 eV) in Figure1. hence we discuss here only intermediate to high energy data. The lone theoretical data reported from low to high energy is from Lee et al. [5]. The total cross section of Lee et al. [5] is obtained by summing their elastic cross sections and absorption cross section beyond 15 eV. The present

SCOP data finds excellent agreement with data of Lee et al. [5] beyond 50 eV below which their data are higher compared to the present data. Theoretical data reported by Antony et al. [7] are much higher compared to our data at 50 eV but this discrepancy decreases with increase in energy and after 200 eV they merge with present data. The experimental data reported by Maddern et al. [4] are slightly lower compared to our data but within experimental uncertainty. There is a lone experimental data set reported by Francis-Staite et al. [3] at 50 eV beyond which no other experimental data is reported. There are only two theoretical data sets at higher energies with which to compare our data; one reported by Lee et al. [4] and other reported by Antony et al. [6]. The results of Lee et al. [4] are lower compared to the present results while those of Antony et al. [6] are higher up to 300 eV beyond which all data tend to merge. There is discrepancy between our data and measured data of Francis Staite et al. [3]. This is attributed to large error (~45%) which arises due to extrapolation of DCS from 20o to 0o and 135o to 180o to obtain the integral cross section as discussed earlier. The discrepancy is more at low energy below 10 eV and above 10 eV there is better agreement with our data.

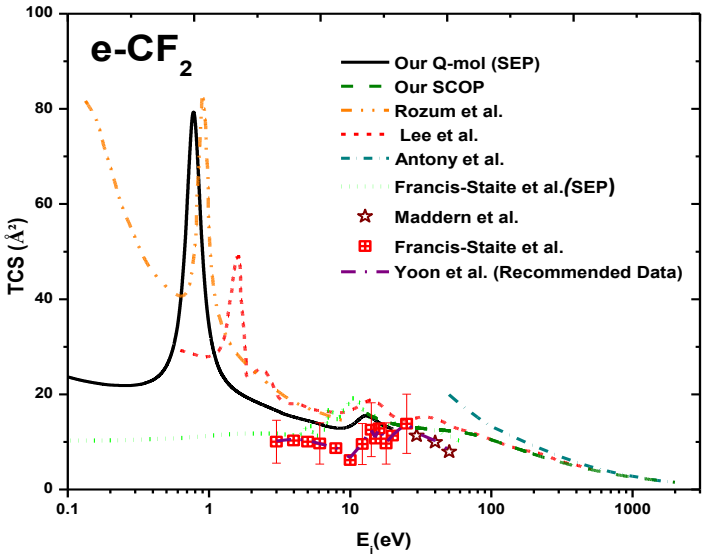

Fig. 2. (Color online) Total cross section for e -CF2 scattering. Black solid line: OurQ-mol results (SEP); Dash dot line: Our SCOP results; Short Dash dot line: Antony et al. [7]; Short Dot: Francis-Staite et al. (SEP) [3]; Dash Dot Dot line: Rozum et al. [6] (SEP); Short Dash line: Lee et al. [5]; Open star: Maddern et al. [4]; Open Square: Francis-Staite et al. [3]; Solid circle: Yoon et al. [45]

Figure 3 shows the eigenphase sum for various doublet scattering states (2A1, 2B1, 2A1 and 2B2) of the CF2 system. It is important to study eigenphase sum as they indicate the position of electron scattering resonances which are important features in low energy regime. Resonances occur when the incident electron is temporarily captured by the target to form a negative ion (an anion) which subsequently decays either by auto detachment (often leaving the target vibrationally / electronically excited) or by dissociating the molecule to produce a net product anion (a process known as Dissociative Electron Attachment (DEA)). A recursive procedure for detecting and performing Breit-Wigner fits to the eigenphase diagram and is done through program RESON [13]. This program generates new energy points and marks those points where the numerically computed values of second derivative changes sign from positive to negative. Finer grids are constructed about each of these points which are used as inputs for Breit-Wigner fit [13] and the two most important parameters (position and width) related to resonances are obtained. Table IV gives the positions and widths of resonances obtained in the our case using R-matrix calculations.

TABLE IV: Position and width of resonance states.

Resonance state	Position (eV)	Width (eV)	Resonance state	Position (eV)	Width (eV)
	Present			Others	
2B1	0.81	0.24	2B1	0.95[6]	0.18[6]
2A1	6.14	---	2A1	5.61[6]	2.87[6]
2B2	13.4	---	2B2	13.5[5]	--
			2B2	15.0[4]	--

The 2B1 state shows a prominent structure in the eigenphase sum which is reflected as a strong peak of 65.59 Å2 in the TCS curve at 1.04 eV and it may be attributed to formation of a 2∏u shape resonance. We also observe resonance structure around 6.14 eV due to 2A1 scattering which is also reflected in our MTCS curve (Figure 6) and this structure is also observed at 5.6 eV by Rozum et al. [6]. The 2B1 excitation cross section also shows an increase around 13.5 eV and this is seen as structure in the TCS curve at 13.4 eV. The 2B2 resonance was reported at 13.5 eV by Francis Staite et al. [3] and same was reported by Lee et al. [5] at 15 eV. No other prominent structures are seen in the eigenphase sum below 14 eV for any symmetry and the same holds true for the total cross section curve. Eigenphase sums also show the important channels to include in the calculations. It is to be noted that as more states are included in the CC expansion and retained in the outer region calculation, the eigenphase sum increases reflecting the improved modeling of Polarization interaction.

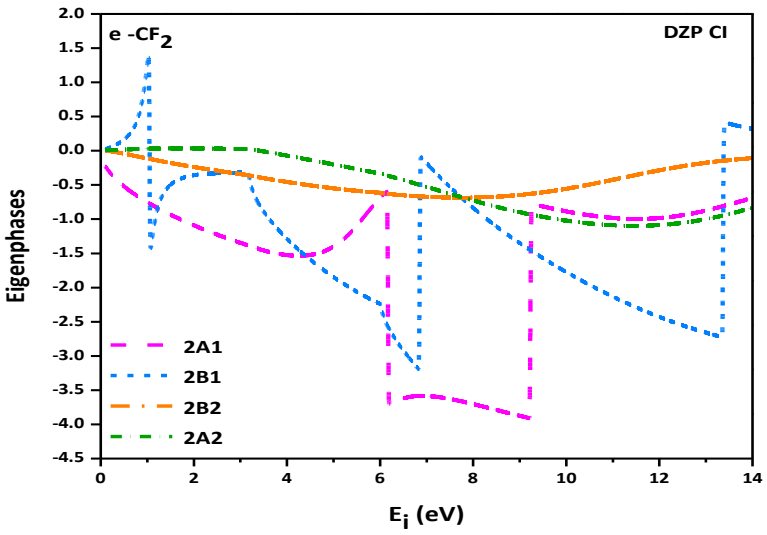

Fig. 3. (Color online) Eigenphase sums of e –CF2 for a 10-state CC calculation.

Figure 4 presents the electronic excitation cross section for excitation of CF2 from the ground state 1A1 to target states 3B1, and 1B1 for incident energies 2 to 10 eV. We have compared the excitation cross sections for first two states with Rozum et al. [6] and have found in general good qualitative agreement except for our excitation cross sections which are quantitatively slightly lower compared to that of Rozum et al. [6]. However the peak position and magnitude remains the same for 3B1 state in our as well as Rozum et al[6] data. From the excitation curve it is evident that first electronic excitation energy for CF2 is at 3.28 eV. The highest contribution to the total excitation cross section comes from the transition 1A1 to 3B1 with a peak of ~1.00 Å2 at 5.8 eV. The transitions beyond 10 eV do not contribute much to the total cross section.

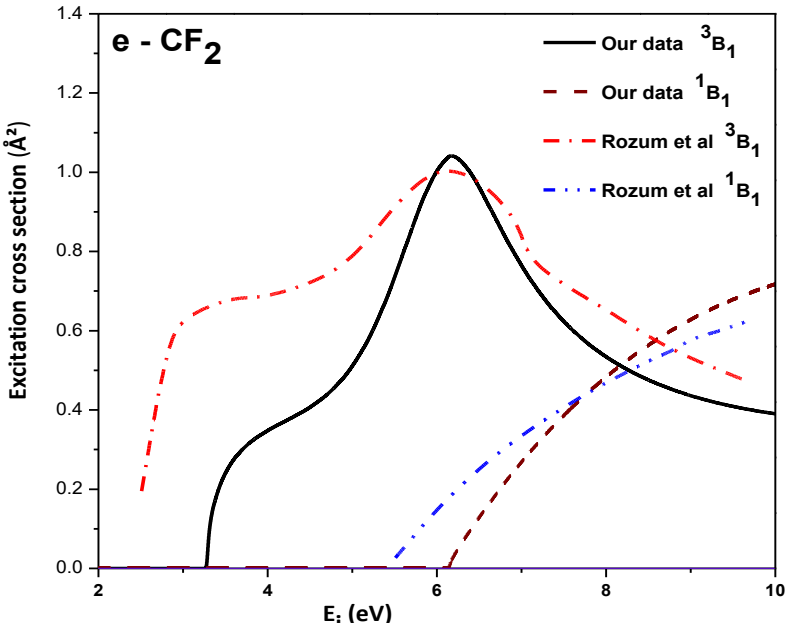

Fig. 4. (Color online) Electronic excitation cross sections of e - CF2 for a 10-state CC calculation from an initial state 1A1.

A study of differential cross sections (DCSs) is very important as they are more accurately measured experimentally, and provide a stringent test for any scattering theory. DCSs are sensitive to effects which are averaged out in the integral cross sections. Hence, we have calculated DCSs for the elastic scattering of electron from CF2 at incident energies 3, 5, 7, 10, 15, and 20 eV over the angular range from 0◦ to 180◦. Figures 5(a) –5(f) show DCSs as a function of angle theta (θ) for incident energies 3, 5, 7, 10, 15, and 20 eV, respectively. We have compared our theoretical data with the other available theoretical results of Rozum et al. [6], Lee et al. [5] and measured data reported by Francis-Staite et al. [3] and observe that present data aer in agreement with available theories but lower compared to the experimental data of Francis-Staite et al. [3].and another observation is that as energy increases, the discrepancies with other theoretical and experimental data decreases and in general a good agreement is observed.

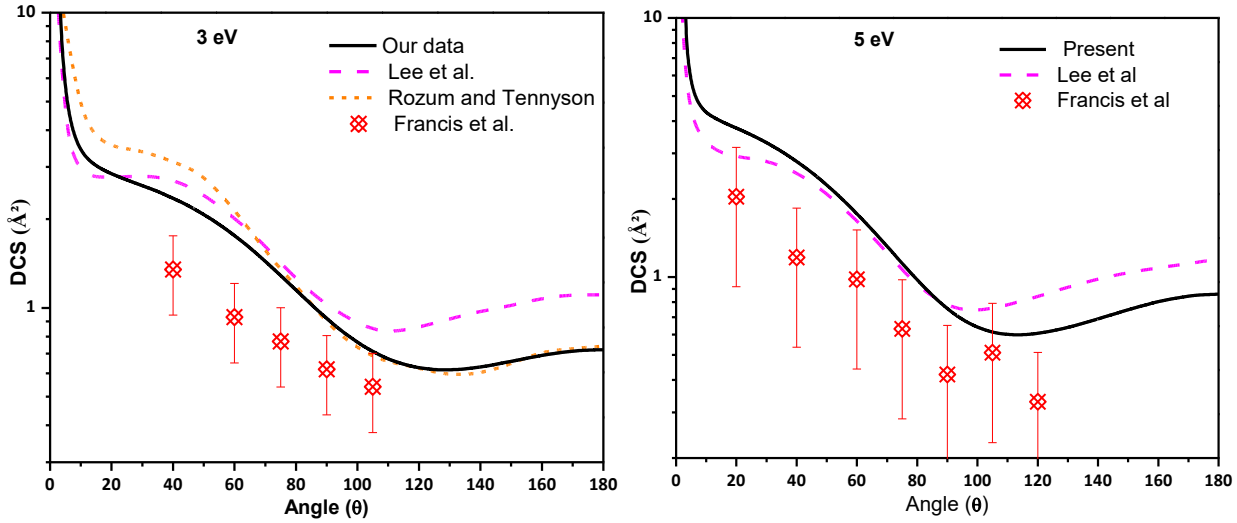

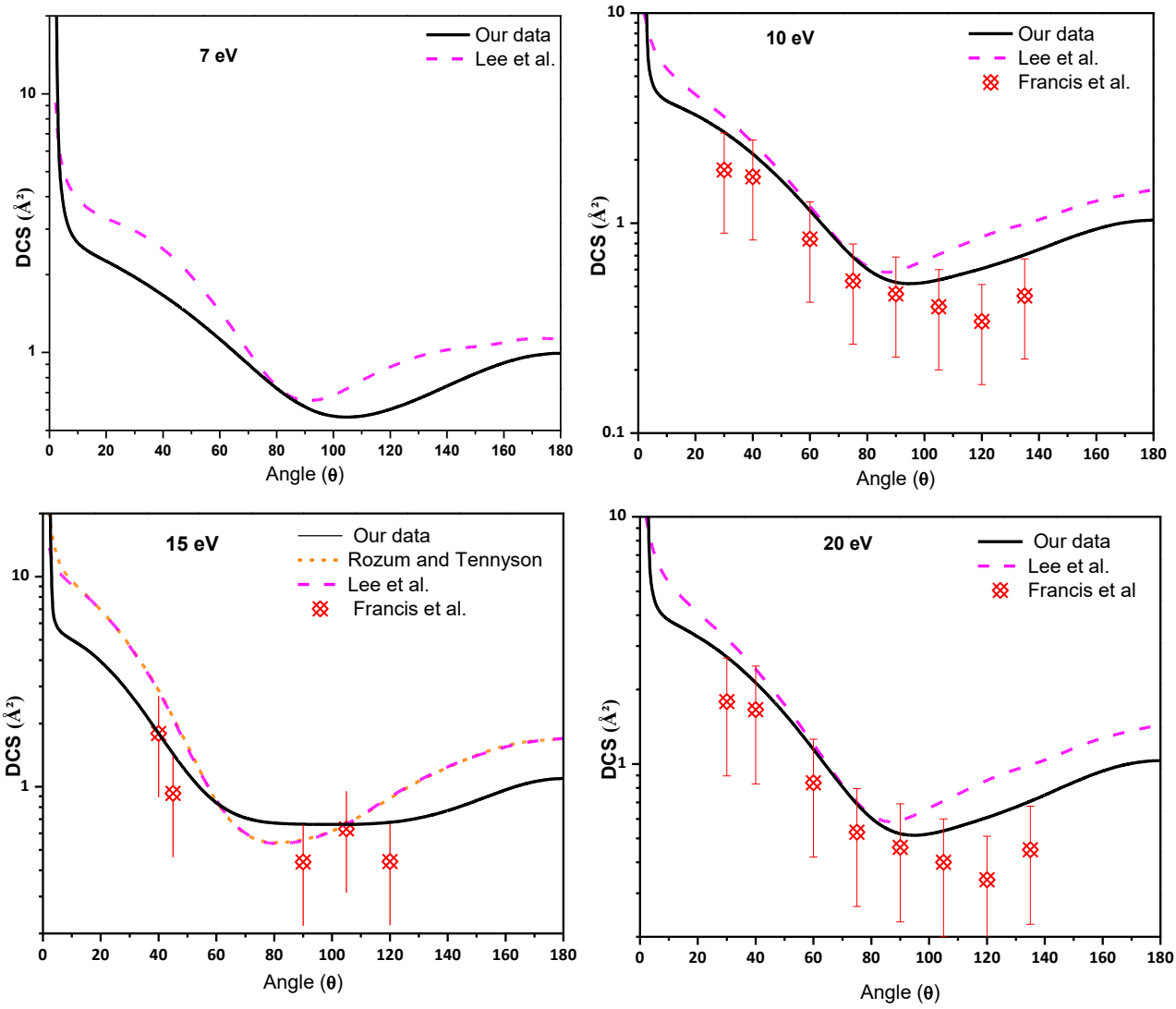

Fig. 5. (Color online) DCS of e – CF2 scattering at (a) 3 eV, (b) 5 eV, (c) 7 eV, (d) 10 eV, (e) 15 eV and (f) 20 eV.

A test on the quality of our DCS is further judged by momentum transfer cross sections (MTCS) as shown in figure 6 for energies 0.01 eV to 10 eV. The MTCS indicate the importance of the backward scattering and is an important quantity that forms the input to solve the Boltzmann equation for the calculation of electron distribution function of swarm of electrons drifting through a molecular gas. In contrast to the divergent behavior of DCS in the forward direction, the MTCS does not diverge due to the multiplicative factor (1 - cosθ). The various peaks or structures observed in MTCS correspond to various resonance processes. Figure 6 shows comparison of present MTCS with theoretical results of Lee et al. [5] and Rozum et al. [6]. Our results show very good agreement with results of Rozum et al. [6] both quantitatively as well as qualitatively except around 6 eV.

The first prominent peak is the reflection of 2B1 scattering which has identical magnitude and position (0.88 eV and 60.01 Å2) as seen in results of Rozum et al. [6] and this peak is also reflected in the TCS (see Figs. 1 & 2). The second peak is at 6.22 eV with magnitude of 16.52 Å2 and it is at 6.77 eV with magnitude of 14.30 Å2 in the results of Rozum et al. [6]. The results of Lee et al. [5] show only one structure and shows shifted first peak compared to our results and the results of Rozum et al. [6] at 1.62 eV with magnitude of 36.85 Å2.

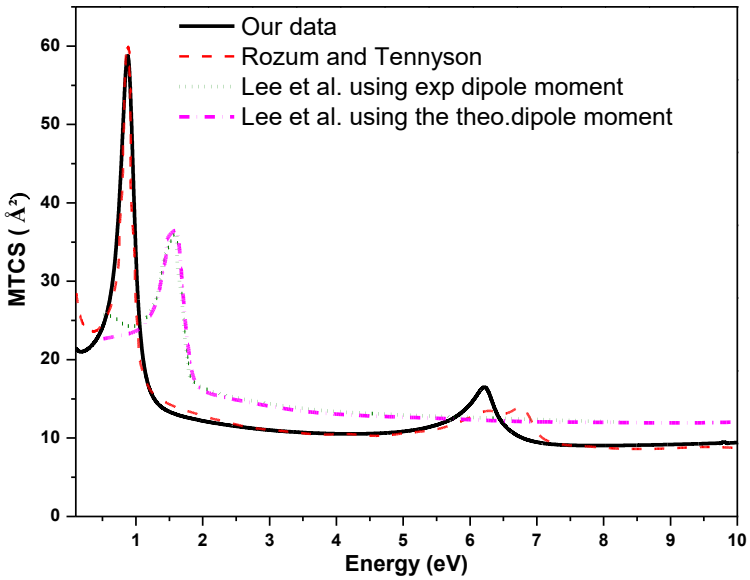

Fig. 6. (Color online) Total momentum transfer cross section for e -CF2 scattering. Black solid line: Our results; Dash Line: Rozum et al. [6]; Short Dot line: Lee et al. [5] using exp. μ; Dash Dot Line using theoretical μ.

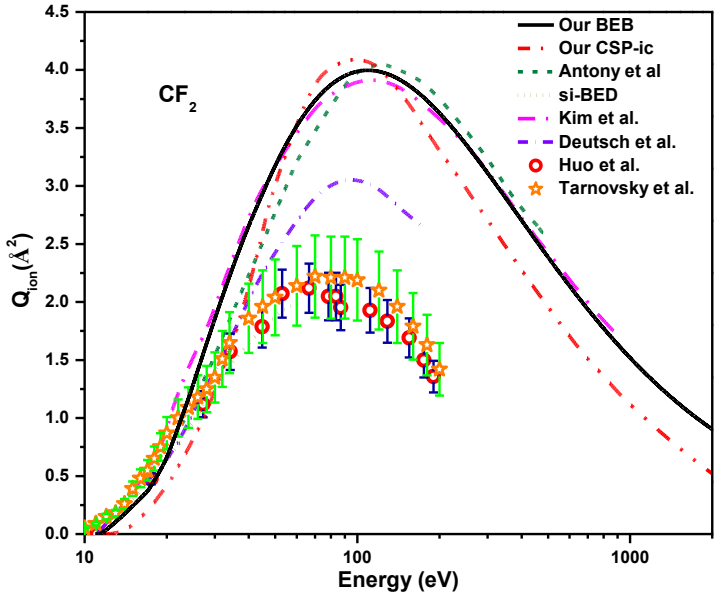

Fig. 7. (Color online) Total ionization cross section for e -CF2 scattering. Black solid line: Our BEB results; Dash Dot Dot line: Present CSP-ic results; Dash line: Antony et al. [7]; Dotted line: si-BED [3]; Dash Dot line: Kim et al. [11]; Short Dash Dot line: Deutsch et al. [10]; Open Circle: Huo et al. [8]; Open circle: Tarnovsky et al. [9]

Finally in Figure 7 we show the comparison of our total ionization cross section of e – CF2 scattering with available results. The theoretical results are reported by three groups [7, 10, 11] and experimentally by two groups [9, 10]. Antony et al. [7] used CSP-ic method, Deutsch et al. [10] used DM formalism and Kim et al. [11] used BEB formalism to calculate total ionization cross section. We have reported total ionization cross sections using CSP-ic method and BEB formalism. The CSP-ic method is described in detail in our earlier publication [35] and hence not repeated here. We find here that experimental data are much lower compared to all theoretical results and have high uncertainty of ~25%. This is due to the fact that CF2 is reactive radical and it has tendency to adhere to the wall of the chamber [3]. All theoretical results are quantitatively and qualitatively in good

agreement with one another except siBED results provided by Deustch et al. [10]. However our CSP-ic data show a peak at same energy as both the experimental results [8, 9] at ~80 eV. Experimental data provided by Huo et al. [8] and Tarnovsky et al. [9] are lower compared to all theoretical data except siBED data [10].

IV CONCLUSIONS

A detailed study of e -CF2 system in terms of eigenphase, electronic excitations, differential cross sections, momentum transfer, ionization and total cross sections has been performed and interaction cross sections are reported in the article. We demonstrate here with the help of eigenphase diagram (Figure 3.) that a CC calculation can give much more information than a simple static-exchange calculation at low energies. We can readily obtain the position of resonances that may arise due to temporary negative ion formation from the eigenphase plots. We obtained a prominent peak of 70.20 Å2 at 0.81 eV for SEP model and 44.20 Å2 at 1.86 eV for SE model which is reflection of Π_u shape resonance state. This resonance is also reflected in the MTCS curve (Figure 6) at 0.88 eV with magnitude of 60.01 Å2. We also observed another small structure at 13.4 eV in our low energy total cross section results which is also seen at the same energy in the data of Lee et al. [5]. This structure is also reflected in the experimental result of Francis–Staite et al. [3] at 10.35 eV. This is due to 2B2 scattering.

We have performed close coupling calculations employing the UK molecular R-matrix code below the ionization threshold of the target while the SCOP formalism is used beyond it [46 – 49]. We have demonstrated through Figures 1and 2 that results obtained using these two formalisms are consistent and show a smooth transition at the overlap energy (~14 eV). This confirms the validity of our theories and hence enables us to predict the total cross sections from low energy (0.1 eV) to high energy (2000 eV).

CF2 is a moderately studied target both by theoreticians and experimentalists for reasons discussed earlier. Hence we have chosen this target so that present methodology may be put to the test while still benchmarking our results by comparing with previous works. From the results presented here we conclude that our results are in good agreement with available data. Therefore, we are confident that this methodology may be employed further to calculate total cross sections over a wide range of impact energies in other molecular systems where experiments are difficult or impossible to perform. Total cross section data is important in a variety of applications from aeronomy to plasma modeling. Accordingly such a methodology maybe built into the design of online databases to provide the ‘data user’ with the opportunity to request their own set of cross sections for use in their own research. Such a prospect will be explored by the emerging Virtual Atomic and Molecular Data Centre (VAMDC) [50].

REFERENCES

1. P. Chabert, H. Abada, J. -P. Booth, and M. A. Lieberman, J. Appl. Phys. 94, 76 (2003)
2. T. Nakano and H. Sugai, J. Phys. D Appl. Phys. 26, 1909 (1993)
3. J. R. Francis-Staite, T. M. Maddern, M. J. Brunger, S. J. Buckman, C. Winstead, V. McKoy, M. A. Bolorizadeh, and H. Cho, Phys. Rev. A 79, 052705 (2009)
4. T. M. Maddern, L. R. Hargreaves, J. R. Francis-Staite, M. J. Brunger, S. J. Buckman, C. Winstead and V. McKoy, Phys. Rev. Lett. 100, 063202 (2008)
5. M. -T. Lee, I. Iga, L. E. Machado, L. M. Brescansin, E. A. y Castro, and G. L. C. de Souza, Phys. Rev. A 74, 052716 (2006)
6. I. Rozum, P. Lima˜o-Vieira, S. Eden, J. Tennyson, and N. J. Mason, J. Phys. Chem. Ref. Data, 35, 267 (2006)
7. B. K. Antony, K. N. Joshipura, and N. J. Mason, J. Phys. B: At. Mol. Opt. Phys. 38, 189 (2005)
8. W. M. Huo, V. Tarnovsky and K. H. Becker, Chem. Phys. Lett. 358, 328 (2002)

9. V. Tarnovsky, P. Kurunczi, D. Rogozhnikov and K. Becker, Int. J. of Mass Spectrom. and Ion Pro. 128, 181 (1993)
10. H. Deutsch, T. D. Meark, V. Tarnovsky, K. Becker, C. Cornelissen, L. Cespiva, and V. Bonacic-Koutecky, Int. J. Mass Spectrom. Ion-Process. 137, 77, (1994)
11. Y.-K. Kim and K. K. Irikura, Proceedings of the 2nd International Conference on Atom Molecular Data and their Applications, edited by K. Barrington and K. L. Bell, AIP Conf. Proc. No. 543 p. 220 (AIP, New York, 2000)
12. I. Schneider, Adv. At., Mol., Opt. Phys., 1994, 33,183.
13. J. Tennyson, Phys. Rep. 491, 29 (2010)
14. A. Jain, J. Chem. Phys. 86, 1289 (1987)
15. L. E. Machado, R. T. Sugohara, A. S. dos Santos, M.-T. Lee, I. Iga, G. L. C. de Souza, M. G. P. Homem, S. E. Michelin, and L. M. Brescansin, Phys. Rev. A 84, 032709 (2011)
16. J. Tennyson, D. B. Brown, J. M. Munro, I. Rozum, H. N. Varambhia, and N. Vinci, J. Phys.: Conf. Ser. 86, 012001 (2007)
17. See http://cccbdb.nist.gov/.
18. N. Russo, E. Sicilia, and M. Toscano, J. Chem. Phys. 97, 5031 (1992)
19. Z. -L. Cai, J. Phys. Chem., 97, 8399 (1993)
20. B. I. Schneider and T. N. Rescigno, Phys. Rev. A 37, 3749 (1988)
21. W. H. Kirchhoff, D. R. Lide Jr, and F. X. Powell, J. of Mol. Spec., 47, 491498 (1973)
22. K. Takatsuka and V. McKoy, Phys. Rev. A 30, 1734 (1984)
23. H. D. Meyer, Chem. Phys. Lett. 223, 465 (1994)
24. C. J. Noble and R. K. Nesbet, Comput. Phys. Commun. 33, 399 (1984)
25. A. M. Arthurs and A. Dalgarno, Proc. Phys. Soc. London, Sect. A 256, 540 (1960)
26. A. Faure, J. D. Gorfinkiel, L. A. Morgan, and J. Tennyson, Comput. Phys. Commun. 144, 224 (2002)
27. S. I. Chu and A. Dalgarno, Phys. Rev. A 10, 788 (1974)
28. M. Gailitis, J. Phys. B 9, 843 (1976)
29. J. Tennyson and C. J. Nobel, Comput. Phys. Commun. 33, 421 (1984)
30. N. Sanna and F. A. Gianturco, Comput. Phys. Commun. 114, 142 (1998)
31. M. Vinodkumar, K. N. Joshipura, C. G. Limbachiya, and B. K. Antony, Eur. Phys. J. D 37, 67 (2006)
32. K. N. Joshipura, M. Vinodkumar, C. G. Limbachiya, and B. K. Antony, Phys. Rev. A 69, 022705 (2004)
33. C. F. Bunge, J. A. Barrientos, and A. V. Bunge, At. Data Nucl. Data Tables 53, 113 (1993)
34. M. Vinodkumar, C. Limbachiya, K. Korot, and K. N. Joshipura, Eur. Phys. J. D 48, 333 (2008)
35. M. Vinodkumar, K. Korot, and P. C. Vinodkumar, Int. J. Mass Spectrom. 305, 26 (2011)
36. I. Gradashteyn and I. M. Ryzhik, Tables of Integrals, Series and Products (Academic, New York, 1980)
37. M. Vinodkumar, K. N. Joshipura, C. Limbachiya, and N. Mason, Phys. Rev. A 74, 022721 (2006)
38. A. Jain and K. L. Baluja, Phys. Rev. A 45, 202 (1992)
39. S. Hara, J. Phys. Soc. Jpn. 22, 710 (1967)
40. X. Zhang, J. Sun, and Y. Liu, J. Phys. B 25, 1893 (1992)
41. G. Staszewska, D. W. Schwenke, D. Thirumalai, and D. G. Truhlar, Phys. Rev. A 28, 2740 (1983)

42. G. Staszewska, D. M. Schwenke, and D. G. Truhlar, J. Chem. Phys. 81, 3078 (1984)
43. F. Blanco and G. Garcia, Phys. Rev. A 67, 022701 (2003)
44. C. J. Joachain, Quantum Collision Theory (North - Holland, Amsterdam, 1983)
45. J.-S. Yoon, M.-Y. Song, H. Kato, M. Hoshino, H. Tanaka, M. J. Brunger, S. J. Buckman and H. Cho, J. Phys. Chem. Ref. Data. 39, 033106 (2010)
46. M. Vinodkumar, A. Barot, and B. Antony, J. Chem. Phys. 136, 184308 (2012)
47. M. Vinodkumar and M. Barot, J. Chem. Phys. 137, 074311 (2012)
48. M. Vinodkumar, C. Limbachiya, A. Barot, and N. Mason, Phys. Rev. A 87, 012702 (2013)
49. A. Barot, D. Gupta, M. Vinodkumar, and Bobby Antony, Phys. Rev. A 87, 062701 (2013)
50. M. L. Dubernet, V. Boudon, J. L. Culhane, M. S. Dimitrijevic, A. Z. Fazliev, C. Joblin, F. Kupka, G. Leto, P. Le Sidaner, P. A. Loboda, H. E.Mason, N. J. Mason, C. Mendoza, G. Mulas, T. J. Millar, L. A. Nu˜nez, V. I. Perevalov, N. Piskunov, Y. Ralchenko, G. Rixon et al., J. Quant. Spectrosc. Radiat. Transfer 111, 2151 (2010)